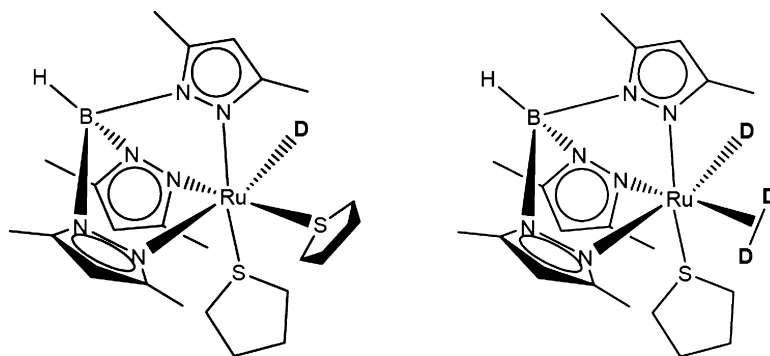


## H Solid-State NMR of Ruthenium Complexes

Bernadeta Walaszek, Anna Adamczyk, Tal Pery, Xu Yeping, Torsten Gutmann, Nader de Sousa Amadeu, Stefan Ulrich, Hergen Breitzke, Hans Martin Vieth, Sylviane Sabo-Etienne, Bruno Chaudret, Hans-Heinrich Limbach, and Gerd Buntkowsky

*J. Am. Chem. Soc.*, **2008**, 130 (51), 17502-17508 • DOI: 10.1021/ja806344y • Publication Date (Web): 19 November 2008

Downloaded from <http://pubs.acs.org> on February 8, 2009



### More About This Article

Additional resources and features associated with this article are available within the HTML version:

- Supporting Information
- Access to high resolution figures
- Links to articles and content related to this article
- Copyright permission to reproduce figures and/or text from this article

[View the Full Text HTML](#)

## $^2\text{H}$ Solid-State NMR of Ruthenium Complexes

Bernadeta Walaszek,<sup>†</sup> Anna Adamczyk,<sup>‡</sup> Tal Pery,<sup>†</sup> Xu Yeping,<sup>†</sup> Torsten Gutmann,<sup>‡</sup>  
Nader de Sousa Amadeu,<sup>‡</sup> Stefan Ulrich,<sup>†</sup> Hergen Breitzke,<sup>‡</sup> Hans Martin Vieth,<sup>||</sup>  
Sylviane Sabo-Etienne,<sup>§</sup> Bruno Chaudret,<sup>§</sup> Hans-Heinrich Limbach,<sup>†</sup> and  
Gerd Buntkowsky<sup>\*,‡</sup>

*Institut für Physikalische and Theoretische Chemie, Freie Universität Berlin,  
Takustr.3, D-14195 Berlin, Germany, Institut für Physikalische Chemie, Friedrich Schiller  
Universität Jena, Helmholtzweg 4, D-07743 Jena, Germany, Laboratoire de Chimie de  
Coordination du CNRS, 205, Route de Narbonne, 31077 Toulouse Cedex 04, France, and  
Institut für Experimentalphysik, Freie Universität Berlin,  
Arnimallee 14, D-14195 Berlin Germany*

Received August 11, 2008; E-mail: gerd.buntkowsky@uni-jena.de

**Abstract:** The  $^2\text{H}$  solid-state NMR spectra of the transition metal complexes  $\text{Tp}^*\text{RuD}(\text{THT})_2$  (**1a**),  $\text{Tp}^*\text{RuD}(\text{D}_2)(\text{THT})$  (**1b**),  $\text{Tp}^*\text{RuD}(\text{D}_2)_2$  (**1c**),  $\text{Cp}^*\text{RuD}_3(\text{PPh}_3)$  (**2**) and  $\text{RuD}_2(\eta^2\text{-D}_2)_2(\text{PCy}_3)_2$  (**3**) have been measured in a wide temperature range. These compounds were chosen as potential model systems for hydrogen surface species in Ru-nanoparticles. The deuterium quadrupolar coupling constants  $Q_{\text{cc}}$  and asymmetry parameters were extracted by  $^2\text{H}$  NMR line-shape analysis. The  $Q_{\text{cc}}$  values of the deuterons bound to the metal vary between 13 kHz and 76 kHz. In addition all spectra show that some of the deuterium is incorporated into carbon positions exhibiting quadrupolar coupling constants in the range of 134 kHz to 192 kHz. The room temperature spectra contain an additional weak very narrow line which was assigned to deuterons exhibiting a high mobility. These deuterons are attributed to crystallographic impurity and partially to  $\text{D}_2$  molecules which lost by the complexes. The temperature where their motion is quenched and the types of these motions depend on the chemical structure. We propose to use the values of the quadrupolar coupling constants measured in order to characterize different hydrogen species on the surface of Ru-nanoparticles.

### 1. Introduction

Recently interest has grown in the chemistry of transition metal nanoparticle materials due to their unique physical and chemical properties. They may be used as catalysts in many organic and inorganic transformations.<sup>1</sup> Many research groups have demonstrated and expanded the methods of their synthesis and investigations, including X-ray diffraction, infrared spectroscopy, neutron scattering, and liquid state nuclear magnetic resonance.<sup>2–7</sup> In the stabilization process of the nanoparticles, ligands like polymers or amino chains are introduced. The main function of these ligands is the prevention of an agglomeration

and precipitation of the metal nanoparticles. Owing to the catalytic activity of the metal surface these stabilizers can also interact with reaction substrates as for example hydrogen/deuterium atoms on the surface of the nanoparticles.<sup>3</sup> The hydrogen atoms exhibit a high mobility on the surface of the metal nanoparticles, which is visible as a change in line shape in solid-state  $^2\text{H}$  NMR spectra of Ru/HAD (hexadecylamine) particles, as reported recently by some of us.<sup>8</sup> The preliminary results published there raised questions about the detailed bonding situation of the hydrogen or deuterium to the Ru surface. This information is available in the  $^2\text{H}$  NMR parameters, particularly in the quadrupolar coupling constant. However, for the interpretation of the value of the quadrupolar coupling constants, reference data on well-defined model systems are necessary.<sup>9,10</sup> Suitable model complexes are transition metal polyhydride, polydihydrogen complexes of the type  $\text{Ru}-\text{D}_n(\text{D}_2)_m$  with ( $n = 0-3$ ,  $m = 0-2$ ). As model compounds for the  $^2\text{H}$  solid-state measurements, we chose to study a set of five selectively  $^2\text{H}$ -labeled ruthenium complexes with different characteristic hydrogen bonding situations (see Scheme 1).

<sup>†</sup> Institut für Physikalische and Theoretische Chemie, Freie Universität Berlin.

<sup>‡</sup> Friedrich Schiller Universität Jena.

<sup>||</sup> Institut für Experimentalphysik, Freie Universität Berlin.

<sup>§</sup> Laboratoire de Chimie de Coordination du CNRS.

(1) Astruc, D., Ed. *Nanoparticles and Catalysis*; Wiley-VCH: Weinheim, 2007.

(2) Narayanan, R.; El-Sayed, M. A. *J. Phys. Chem. B* **2005**, *109* (26), 12663–12676.

(3) Pelzer, K.; Laleu, B.; Lefebvre, F.; Philippot, K.; Chaudret, B.; Candy, J. P.; Basset, J. M. *Chem. Mater.* **2004**, *16* (24), 4937–4941.

(4) Xiaoping, Y.; Hanfan, L.; Kong Yong, L. *J. Mater. Chem.* **2001**, *11*, 3387–3391.

(5) Chaudret, B. *C.R. Phys.* **2005**, *6* (1), 117–131.

(6) Wostek-Wojciechowska, D.; Jeszka, J. K.; Amiens, C.; Chaudret, B.; Lecante, P. *J. Colloid Interface Sci.* **2005**, *287* (1), 107–113.

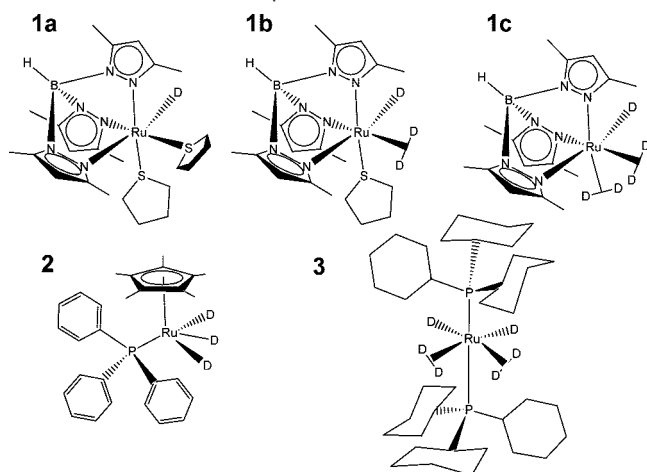
(7) Viau, G.; Brayner, R.; Poul, L.; Chakroune, N.; Lacaze, E.; Fievet-Vincent, F.; Fievet, F. *Chem. Mater.* **2003**, *15*, 486–494.

(8) Pery, T.; Pelzer, K.; Buntkowsky, G.; Philippot, K.; Limbach, H. H.; Chaudret, B. *Chem. Phys. Chem.* **2005**, *6*, 605.

(9) Wehrmann, F.; Fong, T.; Morris, R. H.; Limbach, H.-H.; Buntkowsky, G. *Phys. Chem. Chem. Phys.* **1999**, *1*, 4033.

(10) Facey, G.; Gusev, D.; Macholl, S.; Morris, R. H.; Buntkowsky, G. *Phys. Chem. Chem. Phys.* **2000**, *2*, 935.

Scheme 1. Ruthenium Complexes<sup>a</sup>



<sup>a</sup> (1a) Tp\*RuD(THT)<sub>2</sub>; (1b) Tp\*RuD(D<sub>2</sub>)(THT); (1c) Tp\*RuD(D<sub>2</sub>)<sub>2</sub>; (2) Cp\*RuH<sub>3</sub>(PPh<sub>3</sub>); (3) RuD<sub>2</sub>(D<sub>2</sub>)<sub>2</sub>(PCy<sub>3</sub>)<sub>2</sub>.

From these complexes the quadrupolar coupling constants can be obtained either indirectly by *T*<sub>1</sub> relaxation measurements<sup>11</sup> or directly by <sup>2</sup>H solid-state NMR spectroscopy.<sup>12,13</sup> A recent review about the <sup>2</sup>H solid-state NMR studies of transition metal dihydrogen complexes is given in ref 14. Owing to the fast D/D<sub>2</sub> exchange, which is present even at very low temperatures, resolved *T*<sub>1min</sub> measurements of individual D and D<sub>2</sub> ligands in complexes with several ligands are in general not feasible, and exchange models of the internal D<sub>2</sub> motion are necessary for the determination of the deuterium quadrupolar coupling constants from the relaxation data. By the line-shape analysis of deuterium solid-state NMR spectra the raw quadrupolar coupling constants and asymmetry parameters can be obtained; therefore it has become our technique of choice.

Owing to the high mobility of hydride and dihydrogen ligands in this class of compounds these measurements had to be performed in the temperature range between 10 and 300 K. Employing line-shape analysis of the experimental <sup>2</sup>H solid-state NMR spectra, the quadrupolar coupling constants and their exchange induced changes are elucidated.

The rest of this paper is organized as follows: First, the basics of <sup>2</sup>H NMR line-shape theory are briefly summarized. Then, the syntheses of the model complexes are presented. The experimental section shortly introduces our home-built three-channel NMR spectrometer. Finally, the experimental low-temperature <sup>2</sup>H NMR studies of the ruthenium model complexes are presented, discussed, and summarized.

## 2. <sup>2</sup>H Solid-State NMR

The basic theory of solid-state <sup>2</sup>H NMR is well-documented<sup>15</sup> and only briefly summarized here.

The leading interaction in <sup>2</sup>H solid-state NMR is the quadrupolar interaction. In high field approximation the quadrupolar Hamiltonian of a spin 1 nucleus is given by eq 1:

$$\hat{H}_Q = 2\pi\nu_Q(\vartheta, \phi) \left( \hat{I}_z^2 - \frac{2}{3} \right) \quad (1)$$

where  $\hat{I}_z$  is the angular momentum operator in the *z*-direction. The orientation dependent quadrupolar shift  $\nu_Q$  is given by

$$\begin{aligned} \nu_Q(\vartheta, \phi) &= \pm \frac{3eQeq}{4h} \frac{1}{2} (3 \cos^2 \vartheta - 1 - \eta \sin^2 \vartheta \cos 2\phi) \\ &= Q_{zz} \frac{1}{2} (3 \cos^2 \vartheta - 1 - \eta \sin^2 \vartheta \cos 2\phi) \end{aligned} \quad (2)$$

In eq 2, *eQ* is a quadrupole moment, *eq* represents the principle component of the EFG tensor,  $\eta$  is the asymmetry parameter, which gives information about the shape of the electric field gradient, and *Q*<sub>zz</sub> is a measure for the strength of the quadrupolar interaction;  $\vartheta$  and  $\phi$  are the azimuthal and polar angles of the quadrupolar PAS with respect to the external magnetic field *B*<sub>0</sub>. In a nonoriented powder sample, the average over all possible orientations has to be calculated by integration over the polar angles  $\vartheta$  and  $\phi$ . The quadrupolar coupling *Q*<sub>cc</sub> constant is obtained from the experiment as

$$Q_{cc} = \frac{eQeq}{h} = \frac{4}{3} Q_{zz} \quad (4)$$

## 3. Materials and Methods

**3.1. Sample Preparation.** The synthesis of ruthenium hydride and dihydrogen complexes containing Tp\* = hydridotris(3,5-dimethylpyrazolyl)borate ligands starts with the addition of KTp\* to RuHCl(COD)(bpzm) (bpzm = bis(pyrazolyl)methane). This reaction leads to Tp\*RuH(COD), which is then dissolved in pentane and reacted in a Fischer–Porter bottle with 3 bar of dihydrogen.<sup>16–18</sup> The measurements were performed on three compounds: Tp\*RuD(THT)<sub>2</sub> (THT = tetrahydrothiophene) (1a), Tp\*RuD(D<sub>2</sub>)(THT) (1b), Tp\*RuD(D<sub>2</sub>)<sub>2</sub> (1c) (Scheme 1).

The synthesis of 2 and 3 has been performed using Schlenk techniques. The synthesis of Cp\*RuH<sub>3</sub>(PPh<sub>3</sub>) (Cp\* = C<sub>5</sub>(CH<sub>3</sub>)<sub>5</sub> (1,2,3,4,5-pentamethylcyclopentadienyl)) has been prepared according to Suzuki et al.<sup>19</sup> A slurry of 0.24 g (0.42 mmol) of Cp\*RuCl<sub>2</sub>(PPh<sub>3</sub>) and 0.064 g (1.70 mmol) of NaBH<sub>4</sub> in 10 mL of ethanol was stirred for 24 h at ambient temperature. After evaporation of the solvent the pale brown product was extracted with three portions of 10 mL of toluene. Removal of the solvent from the combined extract under reduced pressure released the ivory microprisms. The yield of obtained prisms was 51% (0.11 g). To obtain Cp\*RuD<sub>3</sub>(PPh<sub>3</sub>) (2) (Scheme 1), the same steps were followed using NaBD<sub>4</sub>.

RuD<sub>2</sub>(η<sup>2</sup>-D<sub>2</sub>)<sub>2</sub>(PCy<sub>3</sub>)<sub>2</sub> (3) (Scheme 1) (Cy = cyclohexyl) was prepared by reacting a pentane solution of Ru(COD)(COT) (COD = 1,5-cyclooctadiene, COT = 1,3,5-cyclooctatriene) and PCy<sub>3</sub> in the presence of dideuterium (3 bar). Then the filtered precipitate was washed with pentane and dried first under a soft argon stream and then shortly in vacuo.<sup>18,20</sup>

**3.2. Spectrometer.** All experiments were performed at a field of 7.03 T corresponding to a <sup>2</sup>H resonance frequency of 46.03 MHz. An Oxford wide bore magnet (89 mm) equipped with a room temperature shim unit was used. The home-built three-channel spectrometer has been described recently.<sup>21,22</sup>

(11) Bakhmutov, V. I.; Bianchini, C.; Maseras, F.; Lledos, A.; Peruzzini, M.; Vorontsov, E. V. *Chem.—Eur. J.* **1999**, *5* (11), 3318–3325.  
 (12) Corti, M.; Pavesi, L.; Rigamonti, A.; Tabak, F. *Phys. Rev. A* **1991**, *43* (12), 6887–6893.  
 (13) Buntkowsky, G.; Limbach, H.-H.; Wehrmann, F.; Sack, I.; Vieth, H. M.; Morris, R. H. *J. Phys. Chem. A* **1997**, *101*, 4679.  
 (14) Buntkowsky, G.; Limbach, H. H. *J. Low. Temp. Phys.* **2006**, *143*, 55–114.  
 (15) Schmidt-Rohr, K.; Spiess, H. W. *Multidimensional Solid State NMR and Polymers*; Academic Press: London, 1994.

(16) Moreno, B.; Sabo-Etienne, S.; Chaudret, B.; Rodriguez, A.; Jalon, F.; Trofimenko, S. *J. Am. Chem. Soc.* **1995**, *117* (28), 7441–7451.  
 (17) Moreno, B.; Sabo-Etienne, S.; Chaudret, B.; Rodriguez-Fernandez, A.; Jalon, F.; Trofimenko, S. *J. Am. Chem. Soc.* **1994**, *116* (6), 2635–2636.  
 (18) Sabo-Etienne, S.; Chaudret, B. *Coord. Chem. Rev.* **1998**, *178–180*, 381–407.  
 (19) Suzuki, H.; Lee, D. H.; Oshima, N.; Morooka, Y. *Organometallics* **1987**, *6* (7), 1569–1575.

For the experiments home-built 5 mm  $^2\text{H}$  NMR probes were used.<sup>23,24</sup> Low-temperature measurements were performed in a dynamic Oxford CF1200 helium flow cryostat. An Oxford ITC 503 temperature controller was used to control the temperature. The typical  $90^\circ$  pulse width was 4.5  $\mu\text{s}$ . A solid echo technique with an echo spacing of 30  $\mu\text{s}$  was used. The repetition time of the experiments was chosen between 1 and 10 s, depending on the  $T_1$  relaxation time of the samples. To acquire the deuterium powder patterns in these samples with a reasonable signal-to-noise ratio, nearly 2000 scans per spectrum were accumulated.

**3.3. Data Evaluation.** Since the measured samples contain several inequivalent deuterons, their spectra are complex superpositions of different subspectra. The shape of these spectra depends on the motional state of the deuterons and changes with temperature. The parameters of the quadrupolar interaction are extracted by line-shape analysis, employing laboratory written Matlab programs which are based on the theory of solid-state  $^2\text{H}$  NMR.<sup>15,25</sup>

Our Matlab program allows one to simulate spectra consisting of up to 8 different subspectra.

For the rigid ruthenium deuterium bond, a nearly axial symmetric quadrupolar tensor is expected. If the deuterium undergoes fast reorientations the value of the quadrupolar tensor and thus also the quadrupolar coupling constants are changed, depending on the type and speed of the motion.

## 4. Experimental Results

Before the presentation of the experimental results some general features of the spectra are discussed. The line shape of the  $^2\text{H}$  NMR spectra depends on the quadrupolar interaction, which is determined by the electric field gradient tensor. Changes of this tensor induce changes of the line shape. In our systems these changes are introduced by the exchange motions of the deuterium ligands. If these exchange motions are frozen, the real value of the quadrupolar interaction is determined. Otherwise an apparent quadrupolar interaction with reduced interaction strength is found.

In particular transition metal hydride complexes can undergo an H/H exchange between the hydride ligand and a hydrogen atom from another ligand, as for example a C–H or  $\text{CH}_2$  group which can come into contact with the metal center.<sup>26</sup> Indeed, the spectra of all model complexes measured and presented in this paper exhibit one additional subspectrum with a  $Q_{zz}$  value between 100 and 144 kHz. This value is characteristic for, possibly, motionally reduced C–D quadrupolar interaction.

As is seen below, the static value of the quadrupolar interaction between ruthenium and deuterium is found for both Ru–D and Ru–D<sub>2</sub> as  $Q_{zz} = 70 \pm 5$  kHz, and the reduced value of the dihydrogen ligands at higher temperatures is in the range 30–42 kHz.

These values are easily distinguishable from the carbon deuterium quadrupolar interaction of deuterated ligands.<sup>12</sup>

The value of the ruthenium deuterium quadrupolar interaction is reduced if the deuterium ligands undergo fast reorientations, for example by chemical exchange. The size and symmetry of the reduced tensor depends strongly on the geometry of the exchange motion and the number of deuterons involved in the exchange process. The exchange rate of the deuterons depends on the temperature and the hindering potential. The latter is much higher for a hydride Ru–D than for a dihydrogen Ru–D<sub>2</sub>. As a consequence of this it is possible to distinguish the two types of deuteron ligands by the temperature dependences of the spectra. At lower temperatures all exchange motions between different ligands will be frozen on the NMR time scale. However, there may still be a coherent quantum exchange of the hydrogens in the dihydrogen ligand.<sup>14</sup> Upon increase of the temperature, first the dihydrogen ligands start to exchange, and only at high temperatures the hydride ligands can also exchange. According to these differences we studied the two pure hydride type complexes **1a** and **2** to determine their quadrupolar coupling constant and three mixed hydride/dihydrogen-type complexes (**1b**, **1c**, and **3**) to reveal the quadrupolar couplings of the dihydrogen ligand.

**4.1. Tp\*RuD(THT)<sub>2</sub> Compound (1a).** All experimentally determined  $^2\text{H}$  NMR parameters are collected in Table 1. In the following for simplicity only the  $Q_{zz}$  values are given.

Figure 1 displays the spectra of sample **1a**, which has only a single hydride ligand, measured at temperatures of 300, 230, and 170 K. The room temperature spectrum consists of a superposition of two strong ( $Q_{zz1} = 100$  kHz,  $Q_{zz2} = 60$  kHz) and one weak ( $Q_{zz3} = 24$  kHz) Pake-like subspectra. In addition, there is a narrow Lorentzian component in the center of the spectrum. The spectrum measured at 230 K can be decomposed into the same Pake-like subspectra with quadrupolar interactions, which have slightly broadened Pake-like subspectra ( $Q_{zz1} = 120$  kHz,  $Q_{zz2} = 68$  kHz,  $Q_{zz3} = 24$  kHz) and a Lorentzian line with weaker intensity as before. At 170 K the Lorentzian line has completely disappeared and only the three Pake-like components ( $Q_{zz1} = 120$  kHz,  $Q_{zz2} = 68$  kHz,  $Q_{zz3} = 24$  kHz) remain in the spectrum. Since the value of  $Q_{zz1} = 120$  kHz is typical for C–D groups of deuterated ligands, the value  $Q_{zz2} = 70$  kHz has to be attributed to the Ru–D group. The assignment of the weak Pake-line with  $Q_{zz3} = 24$  kHz is not completely clear. The most probable explanation is the presence of chemical impurities in the sample.

**4.2. Tp\*RuD(D<sub>2</sub>)(THT) Compound (1b).** Tp\*RuD(D<sub>2</sub>)(THT) includes both a hydride and a dihydrogen type ligand. Figure 2 displays the spectra of sample **1b** measured at 150, 200, and 250 K. At 250 K the spectrum consists of three Pake-like subspectra and a narrow Lorentzian line in the center of the spectrum. The major intensity is in the broadest Pake-like subspectrum ( $Q_{zz1} = 120$  kHz). The other subspectra ( $Q_{zz2} = 62$  kHz,  $Q_{zz3} = 30$  kHz) have weaker intensities. At 200 K the three Pake-like subspectra have slightly broadened ( $Q_{zz1} = 126$  kHz,  $Q_{zz2} = 62$  kHz,  $Q_{zz3} = 36$  kHz), and the narrow line in the center of the spectrum has nearly disappeared. In the spectrum at 150 K only the three Pake-like subspectra ( $Q_{zz1} = 126$  kHz,  $Q_{zz2} = 66$  kHz,  $Q_{zz3} = 40$  kHz) remain. By comparison to the previous section we can assign the broad Pake-like subspectra to the C–D and the 60–70 kHz Pake to the Ru–D groups. It follows that the narrow Pake lines (30–40 kHz) stem from the dihydrogen type ligand Ru–D<sub>2</sub>.

**4.3. Tp\*RuD(D<sub>2</sub>)<sub>2</sub> Compound (1c).** Tp\*RuD(D<sub>2</sub>)<sub>2</sub> contains one hydride and two dihydrogen type ligands (Figure 3). The spectra of this compound are more complex. Five deuterons in

- (20) Borowski, A. F.; Sabo-Etienne, S.; Christ, M. L.; Donnadiou, B.; Chaudret, B. *Organometallics* **1996**, *15*, 1427–1434.
- (21) Buntkowsky, G.; Sack, I.; Limbach, H.-H.; Kling, B.; Fuhrhop, J. J. *Phys. Chem. B* **1997**, *101*, 11265.
- (22) Gedat, E.; Schreiber, A.; Albrecht, J.; Shenderovich, I.; Findenegg, G.; Limbach, H.-H.; Buntkowsky, G. *J. Phys. Chem. B* **2002**, *106*, 1977.
- (23) Wehrmann, F.; Albrecht, J.; Gedat, E.; Kubas, G. J.; Limbach, H. H.; Buntkowsky, G. *J. Phys. Chem. A* **2002**, *106*, 2855.
- (24) Masierak, W.; Emmeler, T.; Gedat, E.; Schreiber, A.; Findenegg, G. H.; Buntkowsky, G. *J. Phys. Chem. B* **2004**, (108), 18890–18896.
- (25) Slichter, C. P. *Principles of Magnetic Resonance*, 3rd ed.; Springer Verlag: Berlin, Heidelberg, New York: 1990.
- (26) Toner, A. J.; Donnadiou, B.; Sabo-Etienne, S.; Chaudret, B.; Sava, X.; Mathey, F.; Le Floch, P. *Inorg. Chem.* **2001**, *40* (13), 3034–3038.



**Table 1.** Parameters Found by the Line-Shape Analysis of <sup>2</sup>H-NMR Spectra ( $Q_{zz}$ , Asymmetry Parameters, Intensities of the Signals, and the Assignments of the Signals)

compd	T [K]	signal	intensity	$Q_{zz} \pm 5$ [kHz]	$\eta \pm 0.001$	$Q_{cc}$ [kHz]	assignments
1a	300	$Q_{zz1}$	$7.91 \times 10^4$	100	0.06	134	C-D
		$Q_{zz2}$	$5.43 \times 10^4$	60	0.06	80	Ru-D
		$Q_{zz3}$	$3.02 \times 10^4$	24	0	32	chemical impurities
1a	230	$Q_{zz1}$	$4.66 \times 10^4$	120	0.06	160	C-D
		$Q_{zz2}$	$5.43 \times 10^4$	68	0.06	91	Ru-D
		$Q_{zz3}$	$1.2 \times 10^4$	24	0	32	chemical impurities
1a	170	$Q_{zz1}$	$4.97 \times 10^4$	120	0.06	160	C-D
		$Q_{zz2}$	$5.26 \times 10^4$	70	0	94	Ru-D
		$Q_{zz3}$	$6.77 \times 10^3$	24	0	32	chemical impurities
1b	250	$Q_{zz1}$	$1.65 \times 10^4$	120	0.1	160	C-D
		$Q_{zz2}$	$3.41 \times 10^3$	62	0.1	83	Ru-D
		$Q_{zz3}$	$5.63 \times 10^3$	30	0.1	40	Ru-D <sub>2</sub>
1b	200	$Q_{zz1}$	$2.25 \times 10^5$	126	0	168	C-D
		$Q_{zz2}$	$5.09 \times 10^4$	62	0.1	83	Ru-D
		$Q_{zz3}$	$6.63 \times 10^4$	36	0.1	48	Ru-D <sub>2</sub>
1b	150	$Q_{zz1}$	$9.13 \times 10^4$	126	0	168	C-D
		$Q_{zz2}$	$3.19 \times 10^4$	66	0.06	88	Ru-D
		$Q_{zz3}$	$2.88 \times 10^4$	40	0.1	54	Ru-D <sub>2</sub>
1c	300	$Q_{zz1}$	$4.81 \times 10^6$	140	0.04	187	C-D
		$Q_{zz2}$	$1.15 \times 10^6$	70	0.04	94	Ru-D
		$Q_{zz3}$	$1.13 \times 10^7$	34	0.05	46	Ru-D <sub>2</sub>
1c	65	$Q_{zz1}$	$1.61 \times 10^7$	142	0.06	190	C-D
		$Q_{zz2}$	$1.23 \times 10^7$	74	0.04	99	Ru-D
		$Q_{zz3}$	$3.51 \times 10^7$	42	0.05	56	Ru-D <sub>2</sub>
1c	30	$Q_{zz1}$	$9.65 \times 10^5$	140	0.045	187	C-D
		$Q_{zz2}$	$3.01 \times 10^5$	76	0	102	Ru-D
		$Q_{zz3}$	$3.96 \times 10^5$	40	0.05	54	Ru-D <sub>2</sub>
1c	10	$Q_{zz1}$	$1.9 \times 10^6$	144	0.1	192	C-D
		$Q_{zz2}$	$1.47 \times 10^6$	70	0.04	94	Ru-D
		$Q_{zz3}$	$1.35 \times 10^6$	42	0.05	56	Ru-D <sub>2</sub>
2	300	$Q_{zz1}$	$4.34 \times 10^8$	56	0	75	Ru-D+Ru-D <sub>2</sub>
		$Q_{zz2}$	$5.49 \times 10^7$	36	0	48	Ru-D <sub>2</sub>
2	250	$Q_{zz1}$	$3.78 \times 10^8$	64	0.1	86	Ru-D
		$Q_{zz2}$	$5.49 \times 10^7$	36	0	48	Ru-D <sub>2</sub>
2	220	$Q_{zz1}$	$1.64 \times 10^9$	68	0.1	91	Ru-D
		$Q_{zz2}$	$3.98 \times 10^7$	18	0.1	24	Ru-D <sub>2</sub>
2	90	$Q_{zz1}$	$3.96 \times 10^8$	70	0.09	94	Ru-D
		$Q_{zz2}$	$1.08 \times 10^9$	22	0.01	30	RuD <sub>2</sub> (D <sub>2</sub> ) <sub>2</sub>
3	300	$Q_{zz1}$	$2.33 \times 10^8$	116	0.04	155	C-D
		$Q_{zz2}$	$1.08 \times 10^9$	22	0.01	30	RuD <sub>2</sub> (D <sub>2</sub> ) <sub>2</sub>
3	200	$Q_{zz1}$	$2.85 \times 10^8$	120	0.04	160	C-D
		$Q_{zz2}$	$9.67 \times 10^8$	26	0.01	35	RuD <sub>2</sub> (D <sub>2</sub> ) <sub>2</sub>
3	150	$Q_{zz1}$	$6.66 \times 10^8$	120	0.04	160	C-D
		$Q_{zz2}$	$1.01 \times 10^9$	28	0.05	38	RuD <sub>2</sub> (D <sub>2</sub> ) <sub>2</sub>
		$Q'_{zz2}$	$2.91 \times 10^8$	42	0.08	56	Ru-D <sub>2</sub>
3	60	$Q_{zz1}$	$2.23 \times 10^8$	122	0.04	163	C-D
		$Q'_{zz2}$	$6.18 \times 10^8$	66	0.1	88	Ru-D
		$Q'_{zz2}$	$1.75 \times 10^8$	42	0.01	56	Ru-D <sub>2</sub>

the compound enhance the ability to incoherent exchange and the complexity of the dynamics. Therefore, a much broader temperature range for the measurements had to be chosen than in the previous samples, and we studied this compound between 10 and 300 K. At room temperature the spectrum consists of three Pake-like subspectra ( $Q_{zz1} = 140$  kHz,  $Q_{zz2} = 70$  kHz,  $Q_{zz3} = 34$  kHz) and a narrow Lorentzian line in the center of the spectrum. The major intensity is in the narrow Pake-like subspectrum. At 65 K the spectrum is again a superposition of three Pake-like subspectra ( $Q_{zz1} = 142$  kHz,  $Q_{zz2} = 74$  kHz,  $Q_{zz3} = 42$  kHz) and a small narrow central line. The relative intensity of the subspectrum with  $Q_{zz2} = 74$  kHz has increased compared to the previous spectra, but the narrow Pake subspectrum still dominates the spectrum. The situation changes at 30 K (Figure 3). Now the intensities are similar for all three subspectra ( $Q_{zz1} = 140$  kHz,  $Q_{zz2} = 76$  kHz,  $Q_{zz3} = 40$  kHz). A

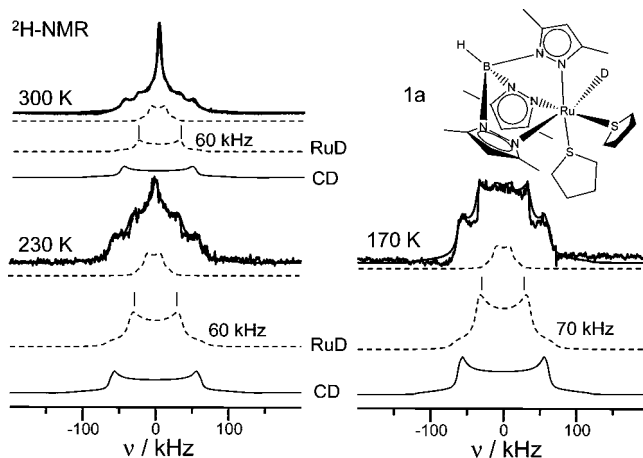


**Figure 1.** Solid-state 46.03 MHz <sup>2</sup>H NMR spectra of Tp\*RuD(THT)<sub>2</sub> (**1a**). The experimental spectra are the sum of the corresponding subspectra (see Table 1).

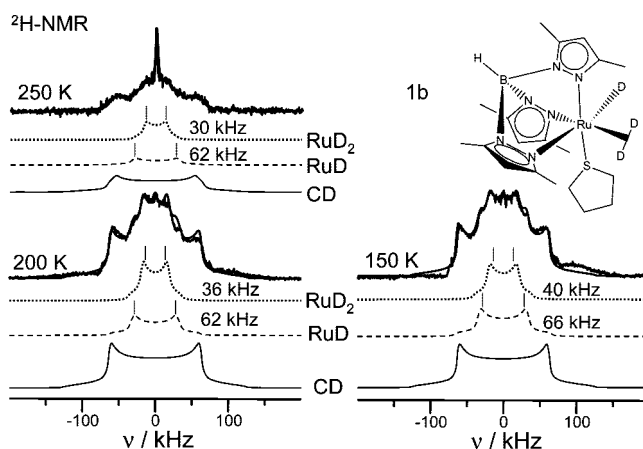


**Figure 2.** Solid-state 46.03 MHz <sup>2</sup>H NMR spectra of Tp\*RuD(D<sub>2</sub>)(THT)<sub>2</sub> (**1b**). The experimental spectra are the sum of the corresponding subspectra (see Table 1).

similar intensity distribution is found in the 10 K spectrum (Figure 3) with three Pake-like lines ( $Q_{zz1} = 144$  kHz,  $Q_{zz2} = 70$  kHz,  $Q_{zz3} = 42$  kHz). According to the previous discussion, the subspectra with  $Q_{zz1} = 144$  kHz and  $Q_{zz2} = 70$  kHz are assigned to C–D and Ru–D groups and the subspectrum with the  $Q_{zz3} = 42$  kHz is assigned to the dihydrogen type ligands.

**4.4. Cp\*RuD<sub>3</sub>(PPh<sub>3</sub>) Compound (2).** The hydride assignments from 4.1 are corroborated by the low temperature spectra of the Cp\*RuD<sub>3</sub>(PPh<sub>3</sub>) complex, which contains three hydride ligands. The room temperature spectrum (Figure 4) consists of two signals, a Pake doublet with  $Q_{zz} = 56$  kHz, and a narrow central line. At 250 K beside a Pake-like subspectrum with a  $Q_{zz}$  of 64 kHz and a very narrow central line, an additional Pake-like subspectrum with a  $Q_{zz}$  of 36 kHz can be seen. Figure 4 presents also the spectrum at 220 K, which contains again three signals, one with a  $Q_{zz}$  of 68 kHz, a second one with a  $Q_{zz}$  of 18 kHz, and a very narrow central line. At 90 K (Figure 4) only one spectrum can be seen with a  $Q_{zz}$  of 70 kHz, which can be attributed to the three deuterium ligands bonded to the ruthenium. The subspectrum with the  $Q_{zz}$  value 36 kHz is discussed in the motional model section (see 5.1) of this complex.

**4.5. RuD<sub>2</sub>(η<sup>2</sup>-D<sub>2</sub>)<sub>2</sub>(PCy<sub>3</sub>)<sub>2</sub> Compound (3).** Figure 5 displays the <sup>2</sup>H NMR spectra of RuD<sub>2</sub>(η<sup>2</sup>-D<sub>2</sub>)<sub>2</sub>(PCy<sub>3</sub>)<sub>2</sub> in the temperature range between 60 and 300 K. At room temperature (Figure 5)

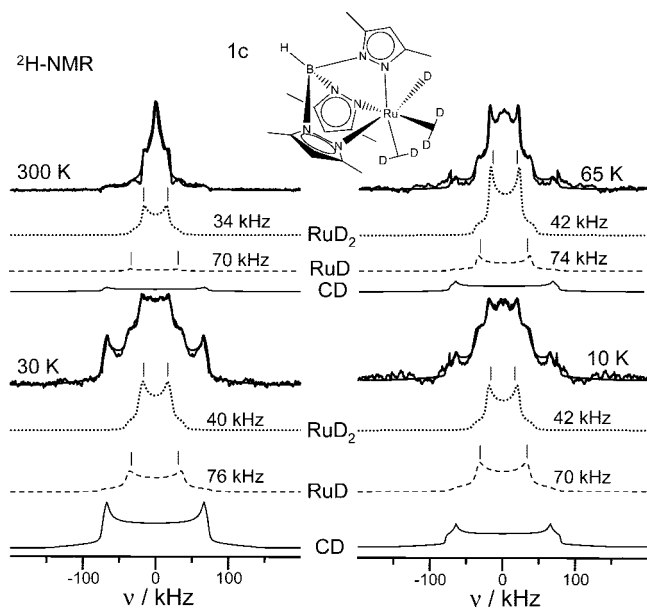


**Figure 3.** Solid-state 46.03 MHz  $^2\text{H}$  NMR spectrum of  $\text{Tp}^*\text{RuD}(\text{D}_2)_2$  (1c). The experimental spectra are the sum of the corresponding subspectra (see Table 1).

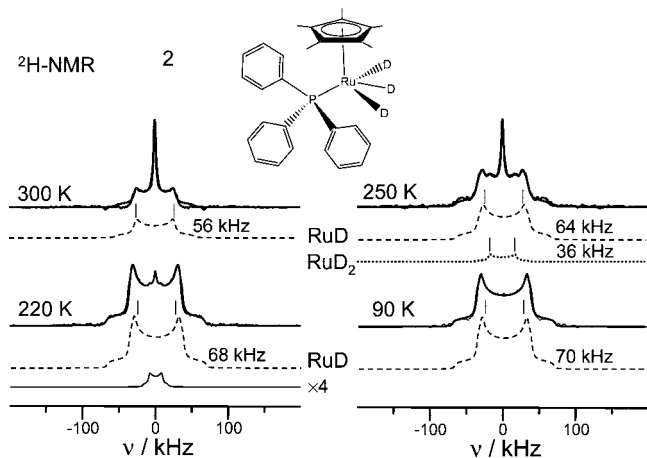


**Figure 4.** Solid-state 46.03 MHz  $^2\text{H}$  NMR spectra of  $\text{Cp}^*\text{RuD}_3(\text{PPh}_3)$  (2). The experimental spectra are the sum of the corresponding subspectra (see Table 1).

the spectrum consists of a superposition of two Pake-like subspectra ( $Q_{zz1} = 116$  kHz,  $Q_{zz2} = 22$  kHz) and a weak narrow component in the center. The major intensity is in the narrow Pake-like subspectrum. The spectrum at 200 K (Figure 5) decomposes into the same subspectra as the room temperature spectrum; however, the strength of the quadrupolar interaction has slightly increased ( $Q_{zz1} = 120$  kHz,  $Q_{zz2} = 26$  kHz) and the intensity of the narrow line in the middle of the spectrum has significantly decreased. At 150 K a third Pake-like subspectrum appears ( $Q_{zz1} = 120$  kHz,  $Q_{zz2} = 28$  kHz,  $Q'_{zz2} = 42$  kHz), and the narrow central line has very small intensity. The 60 K spectrum decomposes into a superposition of three Pake-like subspectra ( $Q_{zz1} = 122$  kHz,  $Q'_{zz2} = 42$  kHz,  $Q''_{zz2} = 66$  kHz), and two narrow lines weakened in intensities.

## 5. Discussion

The  $^2\text{H}$  NMR spectra of five ruthenium model complexes with increasingly complex bonding situations are measured in the temperature range 10 to 300 K. From the temperature depen-

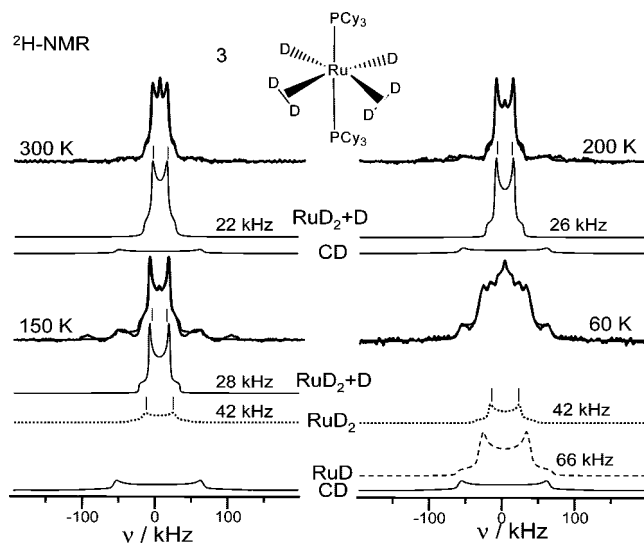


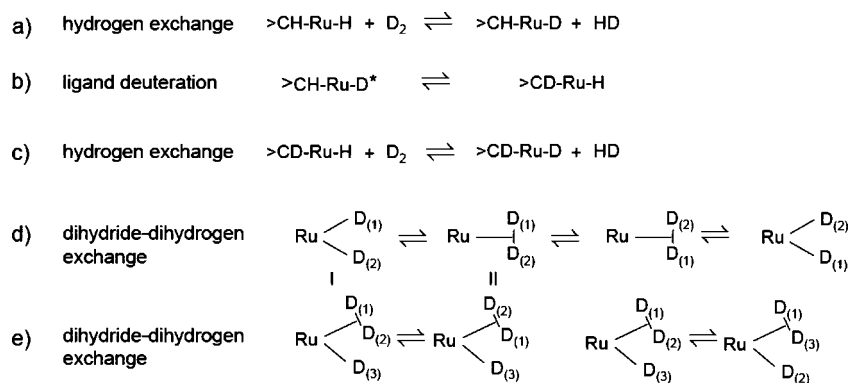
**Figure 5.** Solid-state 46.03 MHz  $^2\text{H}$  NMR spectra of  $\text{RuD}_2(\text{D}_2)_2(\text{PCy}_3)_2$  (3). The experimental spectra are the sum of the corresponding subspectra (see Table 1).

dence of the spectra it is evident that they are strongly influenced by motional and chemical exchange processes. The line-shape analysis of the spectra, employing a superposition of  $^2\text{H}$  Pake patterns and an isotropic line, leads to characteristic values of the quadrupolar interaction. In the following the interpretation of these values in terms of the different bonding situations and mobility of the deuterons is discussed.

**5.1. Motional Models of the Major Species.** As mentioned in the introduction the hydrogen or deuterium atoms in these complexes can perform exchange motions. These motions lead to characteristic changes of the NMR lines shapes, which however are not unique. For this reason a motional model of the different exchange modes have to be developed and the effect of this model on the NMR line shape must be calculated. Before employing these models for the interpretation of the spectra, we shortly discuss the expected motional models for each complex:

**$\text{Tp}^*\text{RuD}(\text{THT})_2$  compound (1a)** is the most simple complex of the studied ones. It contains a single deuterium ligand of the hydride type bound to a ruthenium, two THT ligands, and one  $\text{Tp}^*$  ligand. In this case the deuterium ligand can exchange with hydrogen positions from the organic ligands, causing an isotope scrambling and the formation of C–D groups; moreover it can exchange with  $\text{D}_2$  molecules originating from  $\text{D}_2$  gas impurities (see Scheme 2a and 2b). While the first process is expected to be slow at all temperatures the second might result in a fast exchange regime in the intermediate at elevated temperatures. Accordingly, the spectrum is expected to consist of a broad line of the C–D groups, with a nearly temperature independent line shape and one or two temperature dependent components from the Ru–D and  $\text{D}_2$  deuterons. In this case the chemical exchange between the D and  $\text{D}_2$  type ligands is mainly responsible for the changes in the spectral line shapes and the apparent quadrupolar coupling constants. From the spectra at very low temperatures it is possible to determine the full static value of the quadrupolar coupling constant of the deuteride type Ru–D bond. Comparing these motional possibilities with the experimental spectra shown in Figure 1, we can attribute the broad component with  $Q_{zz} = 130$  kHz to the C–D groups and the narrow component with a 60 to 70 kHz line width to the rigid hydride type Ru–D groups. The variations in the width of the

Scheme 2. Exchange Possibilities for Model Complexes<sup>a</sup>



<sup>a</sup> (a) Hydrogen exchange, (b) ligand deuteration, (c) hydrogen exchange, (d) dihydride–dihydrogen exchange, (e) dihydride–dihydrogen exchange.

C–D and Ru–D line are an indication of vibrational motions of the Ru–D bond, which cause an effective reduction of the size of  $Q_{zz}$ .

**Tp\**Ru*D(D<sub>2</sub>)(THT) compound (1b)** contains one deuteride ligand, one D<sub>2</sub> ligand, one THT ligand, and the Tp\* ligand. The distance  $r_{\text{H-H}}$  between two hydrogen atoms in the H<sub>2</sub> ligand for the Tp\**Ru*H(H<sub>2</sub>)(THT) compound has been calculated using the rapid rotation approximation to be  $\sim 0.89 \text{ \AA}$ .<sup>16</sup> The presence of a dideuterium ligand adds new possible motional modes to the motions discussed above, which are reflected in the spectra: D<sub>2</sub> or H<sub>2</sub> ligands rotate about the M–D<sub>2</sub> axis. This motion is fast and should appear as a contraction of the line shape. Moreover, the chemical exchange between the deuterium ligand and the dideuterium ligand is possible (see Scheme 2e), as well as the exchange of deuterium with hydrogen from other ligands (Scheme 2a and 2c). Therefore, at higher temperatures the coalescence of the line shape is possible. At low temperatures three main subspectra should appear, one for C–D groups and two for D and D<sub>2</sub> ligands. There is also the possibility of producing D<sub>2</sub> gas impurities, when the bond between D<sub>2</sub> ligand and ruthenium is broken.

The weak quadrupolar interaction ( $Q_{zz3} = 30\text{--}40 \text{ kHz}$ ) of the Ru–D<sub>2</sub> dihydrogen ligands is an indication that the fast exchange between the two deuterons of the dihydrogen group has not yet stopped at 150 K.

The assignment of  $Q_{zz2}$  to Ru–D and  $Q_{zz3}$  to Ru–D<sub>2</sub> raises the question of the stoichiometry of the sample. From the stoichiometry one would expect an integral intensity ratio of 1:2 in favor of the D<sub>2</sub> ligands. The line-shape analysis however reveals that both deuteride and dideuterium ligands have comparable intensities. The answer to this puzzle is hidden in the deuteration of the ligands. The dideuterium ligands are chemically far more active than the deuteride ligands and thus preferentially exchange with the ligands. It is interesting to compare the 200 and 250 K spectra. It is evident that the narrow central line has grown strongly in intensity in the 250 K spectrum as compared to the 200 K spectrum. In principle, there are two different interpretations for this, namely either part of the dihydrogen ligands has chemically desorbed from the Ru atom, forming gaseous deuterium (D<sub>2</sub>), or there are chemical impurities in the sample.

**Tp\**Ru*D(D<sub>2</sub>)<sub>2</sub> compound (1c)** contains two D<sub>2</sub> ligands, one D ligand, and the Tp\* ligand. A distance of  $r_{\text{H-H}} \leq 0.90 \text{ \AA}$  has been calculated by Moreno et al.<sup>16</sup> for Tp\**Ru*H(H<sub>2</sub>)<sub>2</sub>, showing that both D<sub>2</sub> ligands are of the dideuterium type. The presence of this second dideuterium ligand again adds new possible

motional modes to the motions discussed above. In particular, one can expect not only a fast planar rotation of dideuterium ligands but also exchange processes between the two dideuterium ligands. When a D<sub>2</sub> ligand leaves the ruthenium, the production of D<sub>2</sub> gas is possible. At low temperatures three different subspectra are expected, one for C–D groups, one for D ligands, and one for D<sub>2</sub> ligands rotating around the M–D<sub>2</sub> axis.

The reduction to  $Q_{zz3} = 42 \text{ kHz}$  of the Ru–D<sub>2</sub> ligand is an indication that the two D<sub>2</sub> ligands are in fast exchange. The theoretical stoichiometry of 1:4 is again distorted because of the deuteration of the ligands.

**Cp\**Ru*D<sub>3</sub>(PPh<sub>3</sub>) compound (2)** contains three deuterium ligands, one PPh<sub>3</sub> ligand, and the Cp\* ligand. The X-ray structure was published by Suzuki et al.<sup>19</sup> This complex is a classical ruthenium trihydride that adopts a four-legged piano-stool structure of C<sub>s</sub> symmetry, with an average Ru–H distance equal to 1.53 Å.<sup>19</sup> Therefore, one mainly expects the same exchange processes as discussed above, i.e. exchange of the deuterides with gaseous D<sub>2</sub>, which could also mediate an indirect exchange in the D<sub>3</sub> system and slow exchange with the organic ligands.

While the assignment of the Pake spectra (Figure 4) with  $Q_{zz} = 64$  to 70 kHz to hydride type Ru–D groups is evident from the comparison to **1a**, the origin of the narrow Pake doublet with  $Q_{zz} = 36 \text{ kHz}$  needs further inspection. According to the results and theoretical calculations published in 1992,<sup>27</sup> the most probable route of exchange between these three deuterium ligands at higher temperatures consists of two steps. In the first step a metastable complex with one D<sub>2</sub> ligand and one D ligand is created, including the rotational tunneling possibility (see Scheme 2d). Therefore, it should be possible to distinguish between these two ligands in this step. The mobility of these deuterium atoms should produce a coalescence of the line shape at higher temperatures. At low temperatures the Pake pattern characteristic for Ru–D bonding should appear. These predictions are in good agreement to the spectra in Figure 4, and we conclude that the Pake doublet with  $Q_{zz} = 36 \text{ kHz}$  is a strong indication of the formation of this metastable state in the trihydride exchange.

**RuD<sub>2</sub>(D<sub>2</sub>)<sub>2</sub>(PCy<sub>3</sub>)<sub>2</sub> compound (3)** exhibits high fluxionality at all temperatures due to six deuterons bonded to the ruthenium.

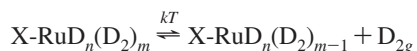
(27) Limbach, H. H.; Scherer, G.; Maurer, M.; Chaudret, B. *Angew. Chem., Int. Ed. Engl.* **1992**, *31*, 1369–1372.

From the X-ray diffraction structure,<sup>28</sup> found for the Ru-(H)<sub>2</sub>(H<sub>2</sub>)<sub>2</sub>(PCy<sub>3</sub>)<sub>2</sub> compound, the distance  $r_{\text{H-H}}$  between the H atoms of the dihydrogen ligand equals 0.86 Å.<sup>28</sup> There have also been measured the Ru–H distances, one between 1.52 and 1.55 Å for the dihydrogen type ligands and the other of 1.70 Å for the hydride atoms. Accordingly, there are two deuteride ligands and two dideuterium ligands. Since a direct exchange of the two deuteride type deuterons would necessitate the breaking of two hydride bonds, one can neglect this process compared to exchange pathways of the dideuterium system and the motional model is similar to the **1c** motional model case. One pathway is a rapid intramolecular deuterium–dideuterium exchange (Scheme 2e), and the other is a rotation of dideuterium ligands. The first one should lead to line coalescence at higher temperatures and can influence the second kind of motion, while the second one causes the characteristic reduction of the quadrupolar coupling constant. At very low temperatures this chemical deuterium–dideuterium exchange should be frozen out and three subspectra should appear in the spectrum (as was observed). One subspectrum is attributed to the deuteride ligands, and the second one to the dideuterium ligands. D<sub>2</sub> ligands exhibit a planar rotation, even at the temperatures below 50 K (as known from INS<sup>18</sup>) causing the narrowing of the signal. The third subspectrum is attributed to the C–D groups.

The reduced  $Q_{zz} = 42$  kHz of the Ru–D<sub>2</sub> ligand indicates that also in this sample the two D<sub>2</sub> ligands are in fast exchange. The theoretical stoichiometry of 1:2 is again distorted because of the deuteration of the ligands.

**Origin of the Narrow Lorentzian Line Component.** The very narrow line, which can be seen in all measured high temperature spectra, can have three possible explanations: (i) it can be caused by chemical impurities in the samples; (ii) it can be caused by a deuterium gas impurities; or (iii) fast isotropic or nearly isotropic motions of the metal bound deuterons cause an isotropic averaging of the deuterium line.

From the preparation of the samples, which involves a reaction step where gaseous hydrogen is applied, it is evident that gaseous D<sub>2</sub> impurities could appear in four of the measured complexes (**1a**, **1b**, **1c**, and **2**). In addition, in the case of the ruthenium dihydrogen complexes **1b**, **1c**, and **3**, the observed temperature dependence could result from the presence of a chemical equilibrium of gaseous D<sub>2</sub> with metal bound deuterium, i.e.



From the temperature dependence it is obvious that the metal bound states are thermodynamically favored as compared to the

gaseous states. In addition, there might be also some physisorption of deuterium gas to the ligands of the complexes that could explain the narrow line in the compound **1a**. The appearance of the weak Pake doublet with  $Q_{zz} = 20$  kHz in each of the spectra of these complexes as well as the lack of any variation of this line with temperature leads to the conclusion of the existence of chemical impurities in these samples.

The possibility of chemically desorbed D<sub>2</sub> from the ruthenium atom can be excluded because that would cause visible chemical changes of the samples. For example, when D<sub>2</sub> desorbs from the RuD<sub>2</sub>(D<sub>2</sub>)<sub>2</sub>(PCy<sub>3</sub>)<sub>2</sub> compound, the color of the sample changes from white to red. Such a color change of the sample was not observed. Chemical impurities are also the most probable explanation for the narrow line in the Cp\*<sup>+</sup>RuD<sub>3</sub>(PPh<sub>3</sub>) complex spectra. In the preparation of this sample NaBD<sub>4</sub> was used. The motion of the four deuterons in the [BD<sub>4</sub>]<sup>−</sup> anion is very fast at high temperatures and gives a narrow line. Therefore, there might be small chemical impurities of NaBD<sub>4</sub> in this compound that cause the appearance of the narrow line in the high temperature spectra.

## 7. Summary and Conclusion

In this work five different Ru complexes are studied by solid-state <sup>2</sup>H NMR spectroscopy in the temperature range 10–300 K. From the line-shape analysis of the spectra the characteristic quadrupolar interactions of the different types of deuterons in the sample are elucidated. It is found that for hydride type Ru–D groups the full, nonmotentially reduced value of the quadrupolar interaction between deuterium and ruthenium is  $Q_{zz} = 70$  kHz, corresponding to a quadrupolar coupling constant of  $Q_{cc} = 94$  kHz. For dihydrogen type ligands, always a coupling reduced by the dihydrogen rotation is found with a typical strength of  $Q_{zz} = 30$ –40 kHz, corresponding to a quadrupolar coupling constant of  $Q_{cc} = 40$ –50 kHz. Thus, it is possible to distinguish between these types of ligands on the basis of their quadrupolar interaction. Moreover we found an experimental indication of a previously proposed metastable transition state in the exchange of a ruthenium trihydride compound. We propose using the deuterium quadrupolar interaction for the characterization of systems with unknown deuterium bonding situations, as for example deuterium adsorbed on Ru nanoparticles, in a similar way as chemical shifts in liquid-state NMR are used to characterize different chemical groups.

**Acknowledgment.** This work has been supported by the CNRS, Toulouse, the Deutsche Forschungsgemeinschaft, Bonn, and the Fonds der Chemischen Industrie, Frankfurt.

JA806344Y

(28) Borowski, A. F.; Donnadiou, B.; Daran, J.-C.; Sabo-Etienne, S.; Chaudret, B. *Chem. Commun.* **2000**, 543–544.